Elsevier Editorial System(tm) for
International Journal of Hydrogen Energy
Manuscript Draft

Manuscript Number: HE-D-20-00874R1

Title: Dispersion of hydrogen release in a naturally ventilated covered car park

Article Type: Full Length Article

Section/Category: Safety / Sensors

Keywords: Unignited release; indoor dispersion; covered car park; release angle; TPRD diameter; natural ventilation.

Corresponding Author: Dr. Sile Louise Brennan, Ph.D

Corresponding Author's Institution: Ulster University

First Author: Harem G Hussein

Order of Authors: Harem G Hussein; Sile Louise Brennan, Ph.D; Vladimir Molkov

Abstract: By necessity hydrogen-powered vehicles will be parked in covered and underground car parks. This has implications for the safety of life and property, and the development of regulations, codes and standards governing passenger vehicles and car parks. This study utilises Computational Fluid Dynamics (CFD) to investigate unignited hydrogen release and dispersion from 700 bar onboard storage in a naturally ventilated covered car park. The impact of leak diameter and angle of leak direction on the formation of the flammable cloud and the implications for vehicle passengers, first responders and car park ventilation are discussed. A typical car park with dimensions LxWxH=30x28.6x2.6 m with two opposing vents based on the British Standard (BS 7346-7:2013) was considered. Releases through three different Thermally Activated Pressure Relief Devices (TPRD) with diameters of 3.34, 2.00 and 0.50 mm were compared, to understand the gas dispersion, specifically the dynamics of envelope formation for 1%, 2% and 4% vol of hydrogen. Concentrations in the vicinity of the vehicle and of the vents were of particular interest. It was shown how blowdown through a TPRD diameter of 3.34 mm leads to the formation of a flammable cloud throughout the majority of the car park space in less than 20 s. However, such a flammable envelope was not observed to the same extent for a TPRD diameter of 2 mm and the flammable envelope is negligible for a 0.5 mm diameter TPRD. A release through a 2 mm TPRD diameter resulted in concentrations of 1% hydrogen along the length of the car park ceiling within 20 s, which should activate hydrogen sensors, in contrast an upward release through a 0.5 mm diameter led to concentrations of 1% reaching a very limited area of the ceiling. Downward TPRD release angles of 0o, 30o and 45o were considered, and while an angle of 30o and 45o directed the hydrogen away from the car body, a downward release at 0o briefly surrounded the car doors and passenger escape routes with a flammable cloud. The study highlights the importance of release angle and demonstrates that a TPRD diameter of 0.5 mm is safer for the particular scenario considered. Larger diameter TPRDs have previously been shown to

be unacceptable from a pressure peaking perspective and this study questions their use safety in a naturally ventilated covered car park.

Highlights

- Hydrogen release from onboard storage in a covered car park is numerically investigated
- Release and dispersions from a range of TPRD diameters is simulated
- A 0.5 mm diameter TPRD was found to be inherently safer for 700 bar storage
- The angle of TPRD release was shown to have implications for passenger egress
- Results support the inherently safe design of hydrogen fuel cell vehicles

Dispersion of hydrogen release in a naturally ventilated covered car park

Hussein H., Brennan S., Molkov V.

Hydrogen Safety Engineering and Research Centre (HySAFER),
Ulster University, Shore Road, Newtownabbey, BT37 0QB, UK.

ABSTRACT

By necessity hydrogen-powered vehicles will be parked in covered and underground car parks. This has implications for the safety of life and property, and the development of regulations, codes and standards governing passenger vehicles and car parks. This study utilises Computational Fluid Dynamics (CFD) to investigate unignited hydrogen release and dispersion from 700 bar onboard storage in a naturally ventilated covered car park. The impact of leak diameter and angle of leak direction on the formation of the flammable cloud and the implications for vehicle passengers, first responders and car park ventilation are discussed. A typical car park with dimensions LxWxH=30x28.6x2.6 m with two opposing vents based on the British Standard (BS 7346-7:2013) was considered. Releases through three different Thermally Activated Pressure Relief Devices (TPRD) with diameters of 3.34, 2.00 and 0.50 mm were compared, to understand the gas dispersion, specifically the dynamics of envelope formation for 1%, 2% and 4% vol of hydrogen. Concentrations in the vicinity of the vehicle and of the vents were of particular interest. It was shown how blowdown through a TPRD diameter of 3.34 mm leads to the formation of a flammable cloud throughout the majority of the car park space in less than 20 s. However, such a flammable envelope was not observed to the same extent for a TPRD diameter of 2 mm and the flammable envelope is negligible for a 0.5 mm diameter TPRD. A release through a 2 mm TPRD diameter resulted in concentrations of 1% hydrogen along the length of the car park ceiling within 20 s, which should activate hydrogen sensors, in contrast an upward release through a 0.5 mm diameter led to concentrations of 1% reaching a very limited area of the ceiling. Downward TPRD release angles of 0^o, 30^o and 45^o were considered, and while an angle of 30^o and 45^o directed the hydrogen away from the car body, a downward release at 0^o briefly surrounded the car doors and passenger escape routes with a flammable cloud. The study highlights the importance of release angle and demonstrates that a TPRD diameter of 0.5 mm is safer for the particular scenario considered. Larger diameter TPRDs have previously been shown to be unacceptable from a pressure peaking perspective and this study questions their use safety in a naturally ventilated covered car park.

KEYWORDS: Unignited release, indoor dispersion, covered car park, hydrogen safety, release angle, TPRD diameter, natural ventilation.

1.0 Introduction

The number of hydrogen-powered vehicles on the roads is growing and it is important to ensure they are at least as safe as conventional vehicles. Onboard hydrogen is typically stored as a compressed gas under high pressure (35 MPa for buses and 70 MPa for cars).

Storage tanks are fitted with Thermally Activated Pressure Relief Devices (TPRD) to release hydrogen, avoiding tank rupture when the surrounding temperature melts the TPRD sensing element at 110^{o} C or above. In the event of a TPRD activation, the released hydrogen might not ignite, instead forming a flammable atmosphere. A fire on the opposite side of the tank for example has potential to cause an unignited release. Failure of a TPRD (which has a non-zero probability) could lead to an unignited release if no measures to ignite the release are taken. The possible subsequent delayed ignition and deflagration event will not be explored in this study which instead focuses on release and dispersion. By necessity, hydrogen vehicles will be parked in garages, underground car parks, present in tunnels, etc. Unignited hydrogen releases in an enclosure have been covered in the literature to a certain extent. However, with the exception of the work by Houf et al. [1], who considered releases from forklifts in warehouses, to date, the emphasis of numerical studies has tended towards low release rates and/or smaller enclosures. For instance, Venetsanos et al. [2] undertook an inter-comparison of CFD models in 2009 to investigate the model capability to reproduce hydrogen dispersion in a garage for a 1 g/s release from a 20 mm leak diameter in a 78.38 m^3 enclosure with two 5 cm diameter vents on one wall. In 2010, Papanikolaou et al. [3] assessed numerically the ventilation requirements for a residential garage with onboard hydrogen storage. In 2013, Bernard-Michel et al. [4] performed an inter-comparison of CFD models for a 4 Nl/min (0.0119 g/s) helium release in a 1 m^3 enclosure with 1 cm circular vent at the base of one wall. Molkov and Shentsov [5] validated the CFD model for buoyant hydrogen releases against the experimental study of Cariteau and Tkatschenko [6] for a laboratory-scale enclosure. When considering unignited releases in an enclosure, both the concentration decay and overpressure may be of interest. Free jets have been previously studied at Ulster and the similarity law and a nomogram is presented in Molkov [7, 8] to calculate hydrogen concentration decay in a momentum-dominated jet. Li et al. [9] numerically investigated unignited and ignited releases from a 4.2 mm diameter TPRD under the car in the open air and it was concluded that the hazard distance for the unignited releases was somewhat longer than those for the ignited release. Previous numerical and analytical work by the authors on unignited releases indoors have been focused on momentum-dominated releases in enclosures with minimum ventilation, leading to the pressure peaking phenomenon [10-13] which is unique for hydrogen (among other fuels). However, in order for the pressure peaking phenomenon to occur the release and enclosure geometry must be such that no air ingress occurs into the enclosure. Whilst this is relevant to residential garages with limited vent(s), the pressure peaking phenomenon will not be caused by releases from typical TPRD diameters in car parks with the minimal ventilation legally required. To date, little or no publications exist on hydrogen unignited releases in car parks. However, it is a topic that has been highlighted as a research gap in a number of publications e.g. [34].

Ventilation recommendations exist to minimise the potential formation of a flammable atmosphere within an enclosure. Ventilation systems should be able to keep hydrogen concentration below the lower flammability limit (LFL) of 4% vol. Indeed, standards typically recommend concentrations do not exceed fractions of the LFL. Standards ISO/DIS 19880-1 [14], NFPA 2 [15] and IEC (60079-10) [16] require that the ventilation rate should ensure a maximum hydrogen mole fraction at 25% of the LFL for enclosures and buildings containing hydrogen equipment, i.e. 1% vol in the case of hydrogen. As an increasing number of car parks are built the majority are constructed in the basement of

residential and commercial buildings [17]. In the literature, both underground car parks and those with two or more sides and a roof are referred to as covered car parks. Previous studies have focused on car fires in a car park and the amount of heat released from such a fire [18]. For example, the smoke movement and fire spread were numerically investigated by Zhang et al. [19] for an underground car park containing three burning cars. Joyeux et al. [20] indicated that the majority of fires in covered car parks involve only one car with the exception of the Schiphol fire accident, where around 10 to 30 cars were engulfed with fire. The difference in ventilation approaches should also be noted, with only wind and buoyancy the influencing factors where natural ventilation is considered. There are no existing studies, either experimental or numerical investigating safety aspects of an unignited hydrogen release in a large confined space such as a naturally ventilated covered car park. The release of hydrogen through a TPRD, dispersion and potential accumulation should be investigated to understand the potential hazards, helping to address potential safety issues. Such an investigation is necessary and in the public interest and hence is the subject of this paper.

2.0 Problem description

A CFD has been used to simulate unignited hydrogen release in a naturally ventilated covered car park. The simulated typical covered car park with dimensions of LxWxH=30x28.4x2.6 m is shown in Fig. 1 (ceiling is not shown). The car park has two ventilation openings: a back vent and front vent, equal in area but differing in shape. The front vent consists of a top to the bottom opening to drive through and two smaller connected side vents near the car park ceiling, representing an area typical of "door with two side vents". In contrast, the back vent is located on the top centre of the back-wall opposite to the front vent. The ventilation requirements were based on BS 7346-7:2013 [21] which states that a covered car park with natural ventilation should have an opening area equivalent to 5% of the floor area for each floor in a level. Similarly, the standard in the Netherlands NEN 2443 [22], requires vents area equivalent to 2.5% of the floor area on each opposite wall (5% in total). The two vents considered were of equal area 21.45 m^2 and located on opposite walls.

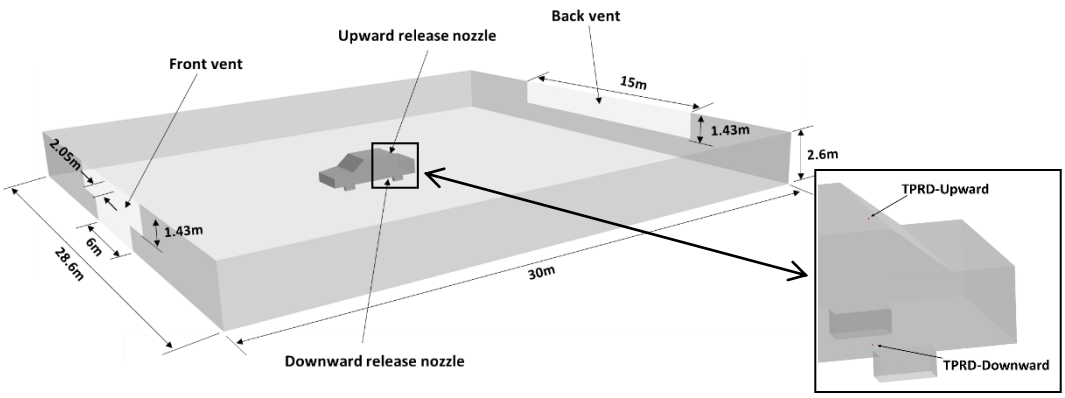

Figure 1. Sketch of the naturally ventilated covered car park with car geometry. Insert highlights TPRD location.

Eleven scenarios were considered varying TPRD diameters and release type, these are listed in Table 1. The non-adiabatic under-expanded jet theory developed at Ulster University [31] was used to calculate the equivalent diameter and parameters of hydrogen for the leak inlet (notional nozzle), thus avoiding the need to resolve the shock structure of the real jet at the TPRD exit. The car volume was not considered in 4 of the 11 cases. This allowed a safer diameter to be determined independent of car geometry. The release in these cases was located exactly at the centre of the car park at a position 0.5 m above the floor. A typical saloon car with dimensions of 4.9 m length, 1.88 m width, and 1.47 m height was chosen. It was assumed that the car was stationary at the time of the leak and the onboard hydrogen tank was filled to capacity. This allows investigation of the worst-case scenario. The hydrogen tank was assumed to have a volume of 117 litres and storage pressure of 70 MPa, with a capacity of approximately 5 kg. It was assumed that the car body is 0.25 m above the ground, with "square" wheels representing the actual equivalent circular diameter.

There are two possibilities for TPRD location: underneath the car close to the rear left the wheel or the upper rear of the car close to back windshield facing upwards. Both locations have been considered in this study, with the TPRD located to the left side of the car with the same horizontal coordinates but differing height, (1.47 m and 0.25 m from the floor respectively). The centre of the leak was situated in the centre of the car park, meaning the car body was positioned slightly left of centre. The ambient temperature and pressure were taken as 293 K and 101,325 Pa respectively, and fully quiescent conditions were considered, i.e. no wind effects, replicating a car park located in an urban setting. While a TPRD release is likely to result in an ignited release the malfunction of a TPRD or activation through impact, warrants investigation, particularly with standard ventilation requirements based on gas concentrations.

Table 1. Scenarios considered for unignited hydrogen release in a naturally ventilated covered car park

Case number	Real release diameter (Notional nozzle diameter) (mm)	Release direction	Angle with vertical axis	Car geometry	Blow-down	Hydrogen mass flow rate (kg/s)
1	3.34 (56.4)	Upward	0^o	**No**	**No**	0.2993
2	3.34 (56.4)	Upward	0^o	**No**	Yes	0.2993*
3	2 (33.8)	Upward	0^o	**No**	Yes	0.1072*
4	2 (33.8)	Downward	0^o	Yes	Yes	0.1072*
5	2 (33.8)	Downward	30^o	Yes	Yes	0.1072*
6	2 (33.8)	Downward	45^o	Yes	Yes	0.1072*
7	0.5 (8.44)	Upward	0^o	**No**	Yes	0.0067*
8	0.5 (8.44)	Upward	0^o	Yes	Yes	0.0067*
9	0.5 (8.44)	Downward	0^o	Yes	Yes	0.0067*
10	0.5 (8.44)	Downward	30^o	Yes	Yes	0.0067*
11	0.5 (8.44)	Downward	45^o	Yes	Yes	0.0067*

* Value at the initial stage, before blowdown.

For TPRDs directed downward it is important to investigate the release angle, as this has a potential impact on the dispersion of the flammable gas with implications for passengers and responders. Angles of 0^o, 30^o and 45^o with the vertical axis were considered as shown in Figure .

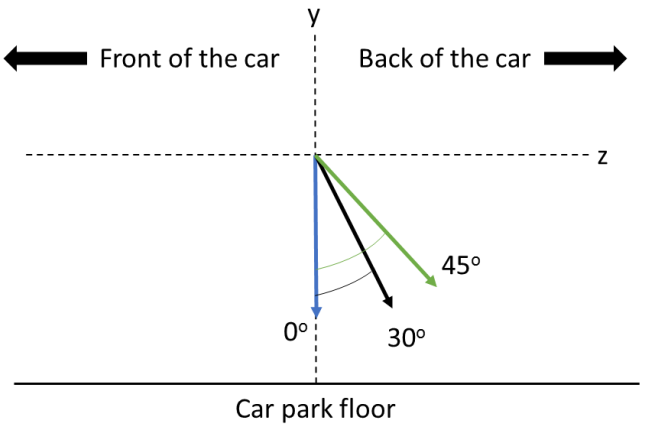

Figure 2. TPRD release angles.

3.0 Model and numerical approach

3.1 Overview

The CFD package ANSYS Fluent [24] was the base software tool used to simulate this high-pressure hydrogen release scenario. Whilst this study is timely and needed to inform the development of RCS, no previous work exists on hydrogen releases in car parks, and as such there is no experimental data. Indeed, there is limited experimental data for high pressure impinging hydrogen jets at a large scale, it is hoped that this work can thus assist in addressing hydrogen safety issues regarding large size enclosures with vents. ICEM CFD was used to generate the geometries and hexahedral meshes, with ANSYS Fluent to solve the governing equations. A pressure-based solver has been used and PISO (Pressure Implicit with the Splitting of Operators) was applied for the transient, compressible flow calculations. Second-order upwind schemes were used for all spatial discretisation, with the exception of the pressure gradient where the PRESTO! interpolation method was applied. A least-squares cell-based approach was used for interpolation methods (gradients).

3.2 Governing equations

The Reynolds-Average Navier-Stokes (RANS) conservation equations were applied to solve for mass, momentum, energy, and species,

$$\frac{\partial \bar{\rho}}{\partial t} + \frac{\partial \bar{\rho}\tilde{u}_j}{\partial x_j} = S_{mass}, \quad (1)$$

$$\frac{\partial(\bar{\rho}\tilde{u}_i)}{\partial t}+\frac{\partial(\bar{\rho}\tilde{u}_i\tilde{u}_j)}{\partial x_j}=-\frac{\partial \bar{p}}{\partial x_i}+\frac{\partial}{\partial x_j}(\mu+\mu_t)\left(\frac{\partial \tilde{u}_i}{\partial x_j}+\frac{\partial \tilde{u}_j}{\partial x_i}-\frac{2}{3}\delta_{ij}\frac{\partial \tilde{u}_k}{\partial x_k}\right)+\bar{\rho}g_i \quad , \tag{2}$$

$$\frac{\partial(\bar{\rho}\tilde{E})}{\partial t}+\frac{\partial}{\partial x_j}\left(\tilde{u}_j\left(\bar{\rho}\tilde{E}+\bar{p}\right)\right)=\frac{\partial}{\partial x_j}\left(\left(k+\frac{\mu_t\, c_p}{Pr_t}\right)\frac{\partial \tilde{T}}{\partial x_j}-\sum_m \tilde{h}_m\left(-\left(\rho D_m+\frac{\mu_t}{Sc_t}\right)\frac{\partial \tilde{Y}_m}{\partial x_j}\right)+\tilde{u}_i\,(\mu+\mu_t)\left(\frac{\partial \tilde{u}_i}{\partial x_j}+\frac{\partial \tilde{u}_j}{\partial x_i}-\frac{2}{3}\,\frac{\partial \tilde{u}_k}{\partial x_k}\,\delta_{ij}\right)\right)+S_E \quad , \tag{3}$$

$$\frac{\partial(\bar{\rho}\,\tilde{Y}_m)}{\partial t}+\frac{\partial}{\partial x_j}\left(\bar{\rho}\tilde{u}_j\tilde{Y}_m\right)=\frac{\partial}{\partial x_i}\left[\left(\bar{\rho}D_m+\frac{\mu_t}{Sc_t}\right)\frac{\partial \tilde{Y}_m}{\partial x_j}\right]+R_m+S_m, \tag{4}$$

where t is the time, ρ is the density, k represents turbulence kinetic energy, μ_t is the turbulent dynamic viscosity, p is the pressure, S_{mass} is the source term which can be added by user define function (UDF), u represents the velocity components, E is the total energy, δ_{ij} is the Kronecker symbol, c_p is the specific heat at constant pressure, g_i is the gravitational acceleration, Sc_t and Pr_t are the turbulent Schmidt and energy turbulent Prandtl numbers, which are 0.7 and 0.85 respectively, Y_m is the mass fraction, D_m is the molecular diffusivity of the species m, S_E are the source terms in the energy equation, R_m and S_m are the net production/consumption rate by species m chemical reaction and the source term connected to any functions defined by the users for dispersed phase.

3.3 Turbulence model

The realizable *k-ε* turbulent model [25] was considered to solve the transport equation for turbulence kinetic energy (k) and turbulent dissipation rate (ε):

$$\frac{\partial(\rho k)}{\partial t}+\frac{\partial}{\partial x_i}(\rho k u_i)=\frac{\partial}{\partial x_i}\left[\left(\mu+\frac{\mu_t}{\sigma_k}\right)\frac{\partial k}{\partial x_i}\right]+G_k+G_b-\rho\,\varepsilon-Y_m+S_k \quad , \tag{5}$$

$$\frac{\partial(\rho\,\varepsilon)}{\partial t}+\frac{\partial}{\partial x_i}(\rho\varepsilon u_i)=\frac{\partial}{\partial x_i}\left[\left(\mu+\frac{\mu_t}{\sigma_\varepsilon}\right)\frac{\partial \varepsilon}{\partial x_i}\right]+\rho C_1 S\varepsilon-\rho C_2\frac{\varepsilon^2}{k+\sqrt{\nu\varepsilon}}-C_{1\varepsilon}\frac{\varepsilon}{k}C_{3\varepsilon}\,G_b+S_\varepsilon \quad , \tag{6}$$

where, Y_m is the contribution of the fluctuating dilatation in compressible turbulence to the overall dissipation rate, G_b and G_k are the buoyancy and the mean velocity gradient respectively, which presents the k generation, ν is the kinematic viscosity, σ_k and σ_ε are the Prandtl numbers of turbulence for k and ε, corresponding to 1 and 1.2. $C_{3\varepsilon}$ is calculated as a function of the flow velocity components with respect to the gravitational vector while C_2 and $C_{1\varepsilon}$ are constants 1.90 and 1.44 respectively. C_1 is evaluated as a function of the modulus of the mean rate of the strain sensor, S. S_k is a source term to be defined by User Define Function (UDF) for Turbulence Kinetic Energy while S_ε represents a UDF source term for turbulence dissipation rate, which was calculated from blowdown parameters via a UDF in this study. This model outperforms the standard κ-ε model especially for calculating spreading rate in axisymmetric jets [24,27].

3.4 Boundary and initial conditions

A domain with outer dimensions LxWxH=170x128.6x92.6 m was used, which is axisymmetric lengthwise. A hexahedral mesh was generated throughout the domain, details of which are given later in this paper. The walls were not meshed. The car park floor, walls, and the roof had a thickness of 0.15 m and were assumed to be constructed of concrete, and the release pipe or car body was considered to be made of aluminium. The material properties chosen are similar to concrete typically used for car parks in the UK and have been used by the authors in previous work [25]. A box mesh technique was implemented to provide a refined mesh around the nozzle and inside the car park, improving resolution without a significant increase in total number of control volumes. A no-slip condition was applied at the solid surfaces. The domain was assumed to be initially 100% air at normal ambient pressure and temperature 101325 Pa and 293 K respectively.

3.5 Notional nozzle model and blowdown process

Hydrogen released from a 70 MPa tank through a TPRD forms an under-expanded jet, leading to a complex shock structure at the nozzle exit, which is computationally intensive to capture. Therefore, the notional nozzle theory developed by Molkov et al. [23, 8] was applied. In addition, the blowdown model developed by Molkov et al. [23] was implemented. Cirrone et al. [28] found that the adiabatic blowdown model provided better agreement with experiment than an isothermal approach for the initial stage of a release, whilst the isothermal blowdown model provided better agreement in the later stages of a release. Thus, an adiabatic blowdown model has been used in this study, as the initial stage of the release is of most interest. Predicted pressure dynamics for blowdown through 3.34 mm, 2 mm and 0.5 mm diameters are shown in Fig. 3. For a TPRD diameter of 3.34 mm on a 117 L tank at 70 MPa, the total blowdown takes over 138 s and the transition from under-expanded jet to expanded jet occurs at 106 s. In contrast, a 0.5 mm diameter TPRD requires 6000 s to fully blowdown and 4742 s to transit to an expanded jet. These differences have to be accounted for by hydrogen tank designers as they affect the required thermal resistance of tank to a fire. It is acknowledged that this presents a significant engineering challenge. Redesign of ventilation systems is also an option. However, this would not eliminate problems associated with existing infrastructure or ignited releases.

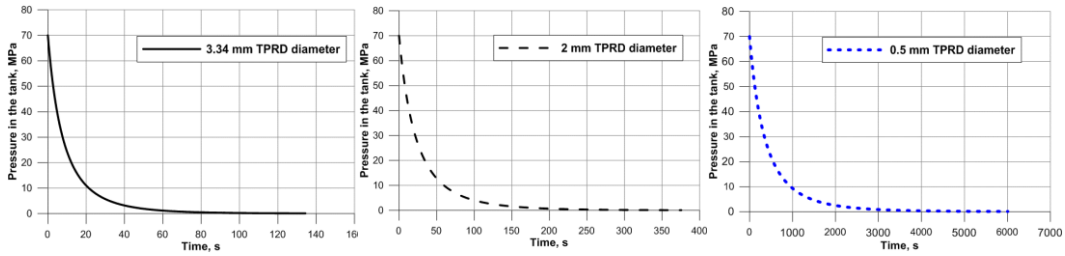

Figure 3. Tank pressure for adiabatic blowdown from 70 MPa. 3.34 mm diameter (left) TPRD; 2 mm diameter TPRD (centre); 0.5 mm diameter TPRD (right).

3.6 Volumetric source model

Decreasing tank pressure during blowdown leads to a corresponding reduction in the notional nozzle diameter. In order to avoid constantly changing the release diameter in the CFD calculation, a volumetric source approach [23] was implemented in a single cell

above the leak. Whilst, greater resolution was considered this was computationally prohibitive. This mimics the hydrogen mass inflow by taking mass, momentum, energy, turbulent kinetic energy and turbulent dissipation energy data from written for Fluent the User Defined Function (UDF). This approach enables changes in the notional nozzle parameters to be reflected in the volumetric sources without any change in the release shape and volume. This method was experimentally validated for hydrogen releases through a 3 mm diameter [29] and the results were presented in detail in [23].

3.7 Grid independency

Three different grids were considered (coarse, intermediate, and refined) to comply with the CFD model evaluation protocols [30]. In each refinement, the average length of the computational cells was halved inside the car park, particularly in areas where high gradients and complex phenomena were expected. Specifically, localised refinement was provided around the hydrogen inlet, the ceiling and regions of the enclosure as recommended [30]. The study was conducted for a constant release through 3.34 mm (case 1) and details are summarised in Table 2. It should be noted that only refinement of the mesh within the car park was changed since the outer domain does not affect conditions in the initial stages of the release. The hydrogen mole fraction was measured at points along the jet axis at increasing height relative to the release, results from a flow time of 0.7 s are shown in Fig. 4 (left). In addition, concentrations were recorded for points 0.021 m under the car park ceiling at an increasing radius from the jet axis, these results at 0.7 s are shown in Fig. 4 (right).

Table 2. Mesh details for grid independence study

Mesh size	No. of cells	No. of faces	No. of nodes
1. Coarse	479,977	1,639,600	532,532
2. Intermediate	691,759	2,302,631	745,416
3. Refine	1,222,412	3,978,771	1,296,276

As seen in Fig. 4 (right) the hydrogen cloud has a radius of 4 m at 0.7 s. The grid independence study showed no significant changes in the results when a coarser grid is used, yet significant savings were made in computational time. Therefore, an “intermediate grid”, was used in the study to achieve a balance between accuracy and computational time. It should be noted that for the example shown, simulation on a refined grid took over 1 month to reach a flow time of 0.7 s. Therefore, it was deemed computationally prohibitive to consider a grid independency study for all diameters.

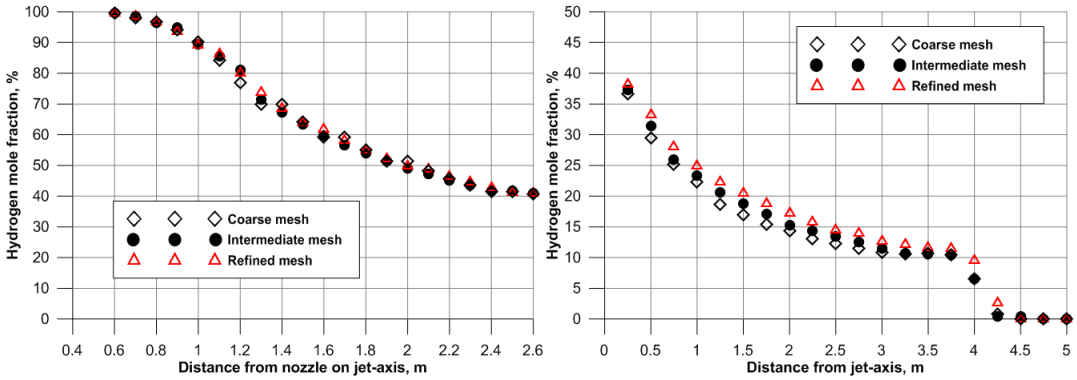

Figure 4. Grid independence study for 3.34 mm TPRD diameter with constant release (case 1) at a flow time of 0.7 s. Hydrogen mole fraction at increasing vertical distance from the leak nozzle along jet axis (left); Hydrogen mole fraction at increasing radial distance from the jet axis at a position 0.021 m under the car park ceiling (right).

4.0 Model validation

As discussed, there is no existing experimental data for a hydrogen release in a covered car park, and limited data exists for impinging unignited jets. However, experimental data for impinging helium jets, produced at KIT-HYKA facility has been considered for comparison. The experiments were carried out within the H2FC European Infrastructure project (http://www.h2fc.eu/) and have not been published in their entirety but are summarised in the work by Dadashzadeh et al. [31]. Helium blowdown from a 19 litre tank at 70 MPa through a release diameter of 1 mm was considered. The release occurred vertically and impinged on to a plate with dimensions 1.52 x 1.51 m. The plate was located 85 cm from the release point. Helium concentration was measured at locations along the surface. Two sensors were considered for validation, as shown in Fig. 5. Concentration measuring probes indicated as Pos 1 and 2 were located 100 mm, and 250 mm from the jet axis respectively.

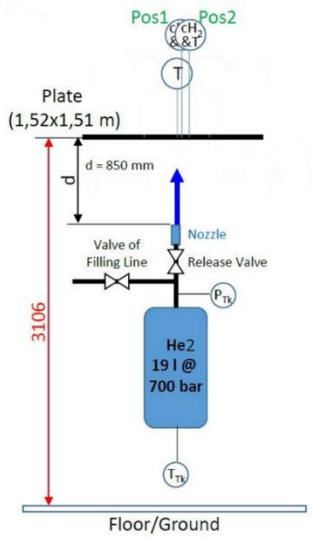

Figure 5. Schematic diagram of KIT experiment for an impinging helium jet [33].

A volumetric source model was employed for the helium release in the CFD simulations. A hexahedral grid was used with refinement in the region of the nozzle area and plate. An indoor environment was considered with dimensions of LxWxH=25.32x7.87x10.42 m. A comparison of the concentration measurements at Pos 1 and Pos 2 is given in Fig. 6 (right). It should be noted that in the experiments, in order to measure concentration, helium gas was suctioned at the plate surface to a helium measuring device along an 80 cm tube, this may be a factor in the time delay observed between the experimental measurements at the beginning of the experiment. Differences between the numerical prediction and the experiment decreased with increasing time.

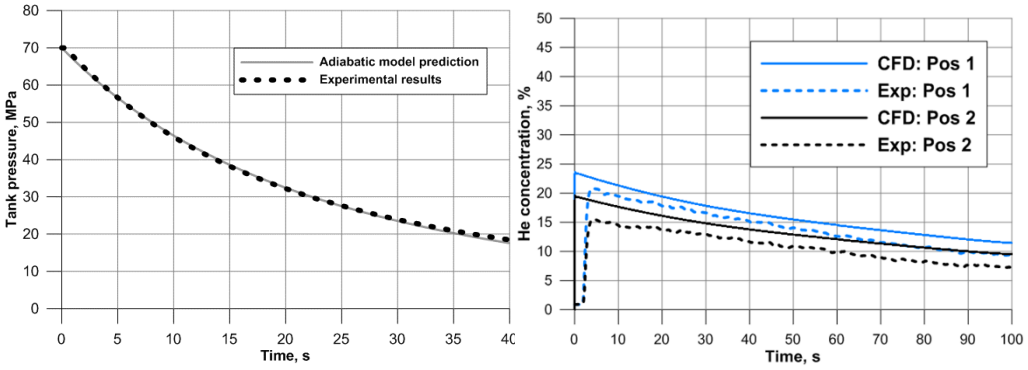

Figure 6. Experimental and adiabatic blowdown model predictions for storage pressure dynamics (left) and experimental and numerical model predictions for helium concentration at plate surface sensors (right).

5.0 Results

Previous studies by the authors have focused on unignited [32] and ignited [10] hydrogen release in enclosures where the aim has been to avoid the hazard and associated risk due to the pressure peaking phenomena. Whereas in this work the larger vents mean that overpressure is not the most significant hazard. Here the focus is on the development of a flammable atmosphere, with a specific emphasis on 1% vol as this represents the maximum allowable mole fraction of hydrogen in an enclosure containing hydrogen equipment in accordance to ISO/DIS 19880-1 [14], NFPA 2 [15] and IEC (60079-10) [16].

5.1 The effect of TPRD diameter on hydrogen dispersion in the car park

Blowdown from 700 bar through a 3.34 mm TPRD diameter was considered as this diameter was also considered in a previous study [25]. Current TPRD diameters can range from 2 to 5 mm, and 3.34 mm was taken as the largest diameter in this study. Whilst this facilitates tank blowdown in a shorter period of time and decreases the risk of tank rupture, the hazards for indoor release, where the gas may accumulate should be considered. Dispersion of hydrogen over the first 60 s of the upward release can be seen in Fig. 7, the iso-surfaces show the extent of the flammable atmosphere (4% vol), and of 25% the LFL (1% vol). A time of 20 s is chosen as it was observed, that with the exception of the

constant mass flow rate release (not blowdown of tank), the flammable envelope was at a maximum at or before 20 s for the three diameters. The emphasis in this study is on extent of the lower concentration envelopes i.e. 1% and 2% as these are relevant to sensor activation and the ventilation systems. An analysis of the potential for delayed ignition, explosion, and the resultant consequences have not been discussed here.

It can be seen that within 20 s there is a hydrogen concentration of 1% vol or higher throughout the enclosure, demonstrating that for the particular release, the natural ventilation (at its conservative conditions of use, i.e. presence of vents in the absence of wind) of the carpark is incapable of maintaining a hydrogen mole fraction below 1%, any hydrogen sensors present would be activated. It can also be seen how a flammable cloud has been formed across the ceiling of the car park within just 10 s of release (with further decrease due to blowdown). This flammable cloud reduces from a maximum at 10 s to only a small volume above the release point by 60 s. The envelope of 1% vol of hydrogen continues to grow filling most of the car park within 60 s of the release. Fortunately, it doesn't imply ignition followed by deflagration hazard unless it is within flammable envelope and the ignition source has enough energy.

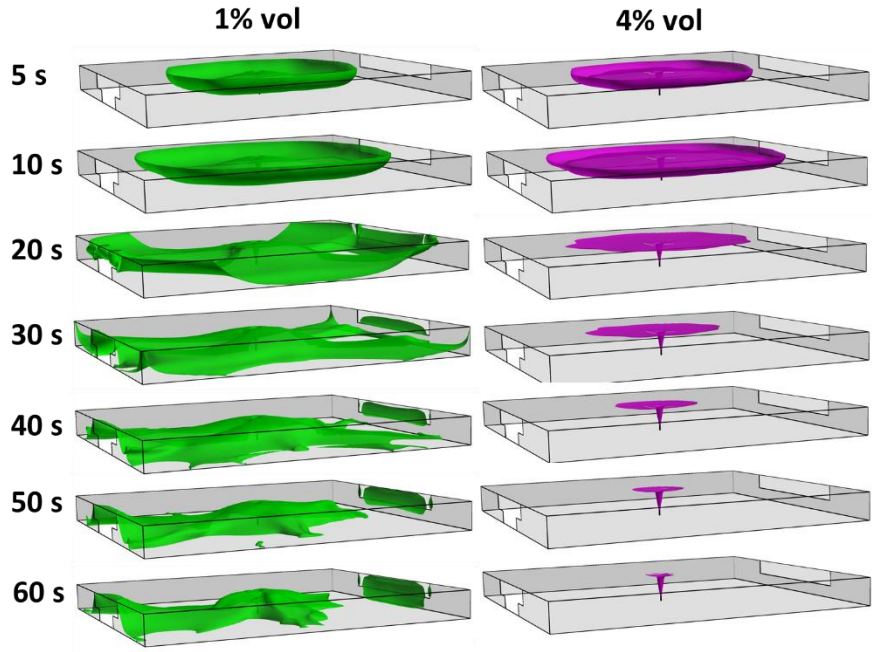

Figure 7. Hydrogen mole fraction for blowdown from 700 bar through a 3.34 mm diameter TPRD for iso-surface 1% vol (left) and 4% vol (right).

Four upward releases were simulated: blowdown through diameters of 3.34 mm, 2 mm, and 0.5 mm, and for comparison a constant release through a 3.34 mm diameter. It should be noted that a constant release through 3.34 mm is unrealistic as both pressure (and hence mass flow rate) will rapidly drop as the tank blows down. However, inclusion of this case allows for comparison with previous work and is also of interest as a conservative worst case scenario as onboard tank capacity and pressure increases going forward.

Iso-surfaces of 1% vol and 2% vol at 20 s can be seen in Fig. 8, and 4% vol in Fig. 9. The effect of accounting for blowdown through the 3.34 mm TPRD can be clearly seen and is most evident in Fig. 9.

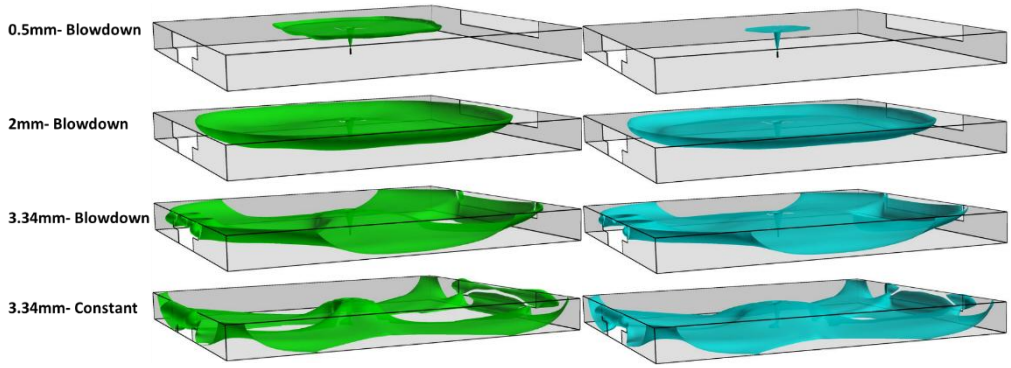

Figure 8. Hydrogen mole fraction after 20 s for upward releases from 700 bar through 0.5 mm (case 7), 2 mm (case 3) and 3.34 mm (case 1 for constant release and case 2 for tank blowdown) diameters for iso-surface 1% vol (left) and 2% vol (right).

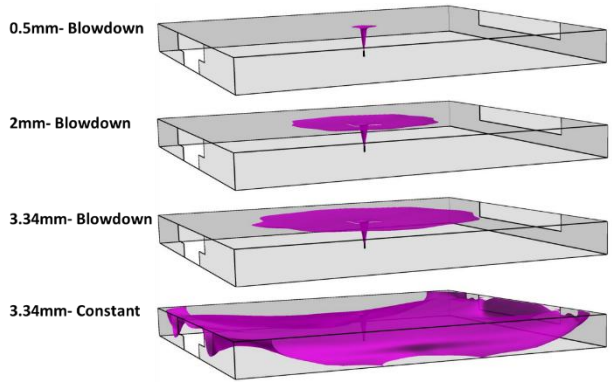

Figure 9. Iso-surface showing 4% hydrogen mole fraction after 20 s for releases from 700 bar through 0.5 mm (case 7), 2 mm (case 3) and 3.34 mm (case 1 for constant release and case 2 for tank blowdown) TPRD diameters.

It can be seen that even when blowdown is accounted for a TPRD diameter of 3.34 mm can lead to some safety concerns, with a flammable atmosphere being formed throughout the car park. In contrast, it is shown how a release through a 2 mm diameter TPRD from 700 bar leads to a much smaller flammable hydrogen cloud around the release nozzle and under the ceiling (and even smaller volume of fast burning mixture of hydrogen, which may imply pressure load, in the range of concentrations 30-42% vol). Concentrations of 1% vol, are predicted in the vicinity of the vents within 20 s. A 2 mm TPRD diameter led to a flammable cloud with a radius of approximately 5 m above the leak and underneath the ceiling.

In the case of the 0.5 mm TPRD diameter it can be seen from Figs. 8 and 9 how a flammable cloud is formed in a very limited area above the leak in contrast with the larger diameters considered. This is in-line with predictions using the similarity law for unignited jets [8], which indicates a maximum concentration of approximately 6% at the ceiling after blowdown of 20s through 0.5 mm from 700 bar. From Fig. 10 (right) it can be seen how the extent of the flammable atmosphere grows only slightly over the initial 20 s of the release. Thus, a TPRD diameter of 0.5 mm could be considered as a safer diameter for unignited hydrogen release from onboard storage in this case. It should be noted that the increased blowdown time associated with the decreased diameter provides additional safety challenges and innovative storage technologies should be investigated. In contrast, the extent of the hydrogen cloud at 1% continues to grow over 20 s, as shown in Fig. 10 (left).

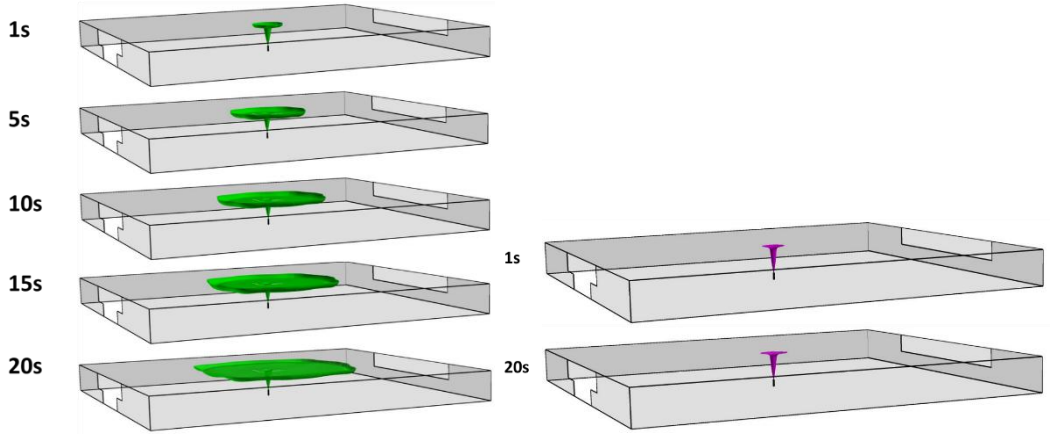

Figure 10. Hydrogen mole fraction for a blowdown release from 700 bar through a 0.5 mm (case 7) TPRD for iso-surface 1% vol (left) and 4% vol (right).

5.2 Comparison between upward and downward hydrogen release

In addition to releasing hydrogen through a “pipe” 0.5 m above the carpark floor, a car body was also considered to represent a more realistic scenario. Two different release directions were considered using a 0.5 mm TPRD diameter to investigate the effect of release orientation and release location. Results for a downward release, from a location under the car beside the rear left wheel, are shown in Fig. 11 for 4% hydrogen mole fraction.

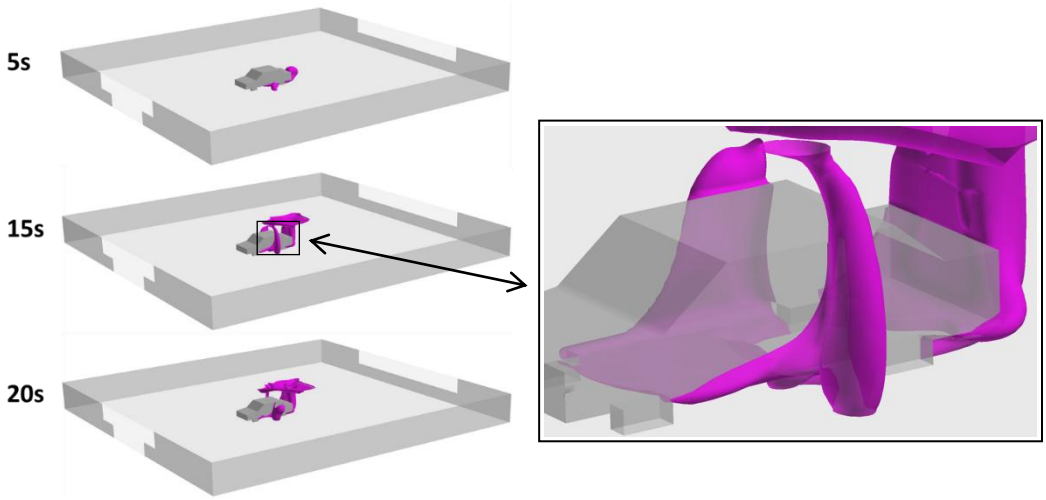

Figure 11. Iso-surface showing 4% hydrogen mole fraction for a downward release from 700 bar through a 0.5 mm (case 9) TPRD diameter.

The maximum flammable envelope was reached at a release time of approximately 15 s, after which time the height of the jets at the sides and rear of the car began to reduce, this height reduction is observed by 20 s. Since the release was downwards, impinging on the floor, the car wheels obstructed the flow dispersion, leading to a non-uniform release pattern. Within 15 s of the release, the flammable envelope covered the rear, left and right of the car in addition to regions of the ceiling. It is acknowledged that the duration is short, and the flammable cloud disperses quickly, this if unignited the position of the flammable gas in the vicinity the car is unlikely to cause alarm. However, the simulation suggests a downward release presents a greater safety concern for access to and from the car, in the case of ignition.

An upward release was also simulated at a height of 1.13 m from the ground, representing the top of the car and the results are shown in Fig. 12 for 4% hydrogen mole fraction. It is noted that the release is at a different height to the downward case however, this is based on positioning the PRD either directly under (downward) or above (upward) the car body.

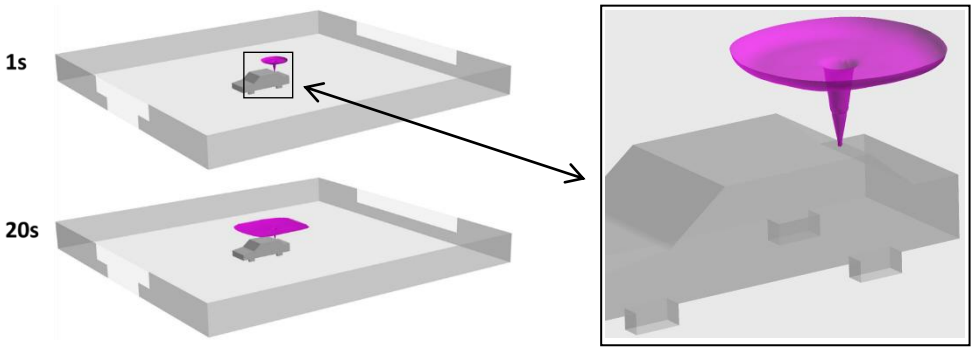

Figure 12 Iso-surface showing 4% hydrogen mole fraction an upward release from 700 bar through a 0.5 mm (case 8) TPRD diameter.

For an upward release the maximum flammable envelope was formed at approximately 20 s, i.e. 5 s later than for the downward case. It can be seen from Fig. 12 how the flammable envelope covers a comparably larger area beneath the ceiling but is spread over a smaller region surrounding the car, and hence has a higher average hydrogen concentration.

A comparison of the gas envelope development for 1% hydrogen mole fraction for a downward and upward release through a 0.5 mm TPRD diameter is shown in Fig. 13. Whilst 1% may not give rise to safety concerns, it is noted that the standards state that H_2 mole fraction should not increase above 1%, mechanical ventilation should be used to ensure this and sensors should be activated. It is seen how for the downward release the envelope of 1% volume is considerably smaller in the region underneath the ceiling, however, the car itself is surrounded on three sides by the gas cloud. In contrast, the upward release led to a relatively larger envelope of 1% hydrogen in the region beneath the ceiling, with a minimal envelope seen in the vicinity of the car. This has implications for sensor position and activation time. It should be mentioned that both downward and upward releases could be classified as safer in this particular scenario if a 0.5 mm TPRD diameter is used because the flammable cloud produced is limited and it disperses quickly. Again, it is noted this requires an increase in tank fire resistance or innovative design. TPRD diameters larger than 0.5 mm can lead to a more significant flammable cloud in the absence of additional ventilation. It should be emphasised that whilst the envelope at 1% vol has not reached a maximum at 1%, the flammable zone has already begun to reduce by this time, as discussed in the previous section.

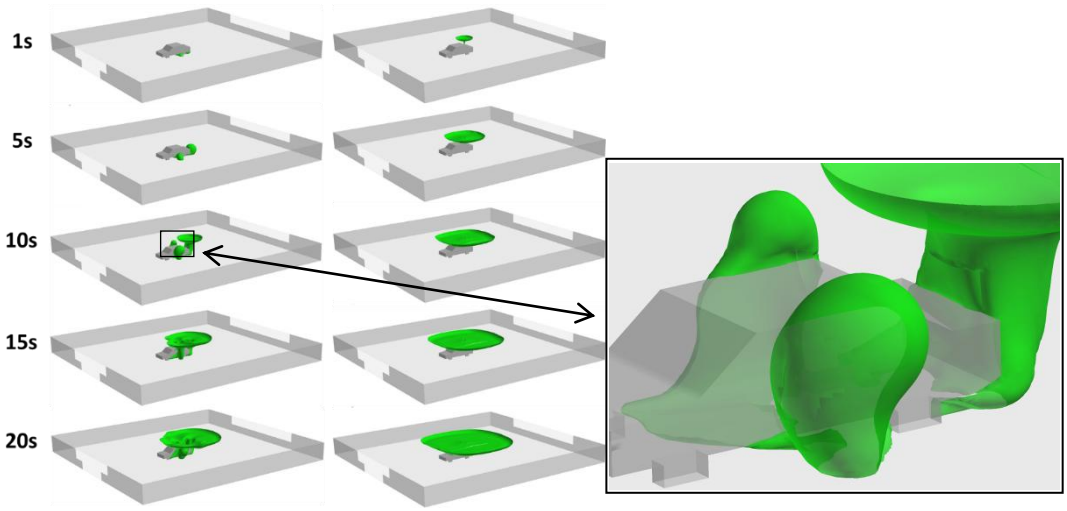

Figure 13. Iso-surface showing 1% hydrogen mole fraction for release from 700 bar through a 0.5 mm TPRD diameter for downward release (case 9) (left) and upward release (case 8) (right).

5.3 The effects of downward release angles

The effect of downward release angles on hydrogen dispersion in a covered car park was investigated for TPRD diameters of 2 mm and 0.5 mm. Three downward release angles of 0^o, 30^o and 45^o with the vertical axis were compared.

Gas envelopes for a downward release at 0^o through a 2 mm are shown in Fig. 14. The car body and vertical downward direction of the release played a role in decreasing the hydrogen flammable cloud under the ceiling. Concentrations of 1% vol and higher are observed around the car and below the ceiling in 40 s, with the gas cloud at 1% vol expected to grow further with time. The flammable hydrogen cloud (4% vol) covers the passenger and driver escape routes, and almost half of the car park ceiling. An iso-surface at 8% vol represents the lower flammability limit of downward flame propagation [9] and hence is included to provide insight. The gas cloud at 8% vol hydrogen reached its maximum coverage area in just 30 s after which point it reduces.

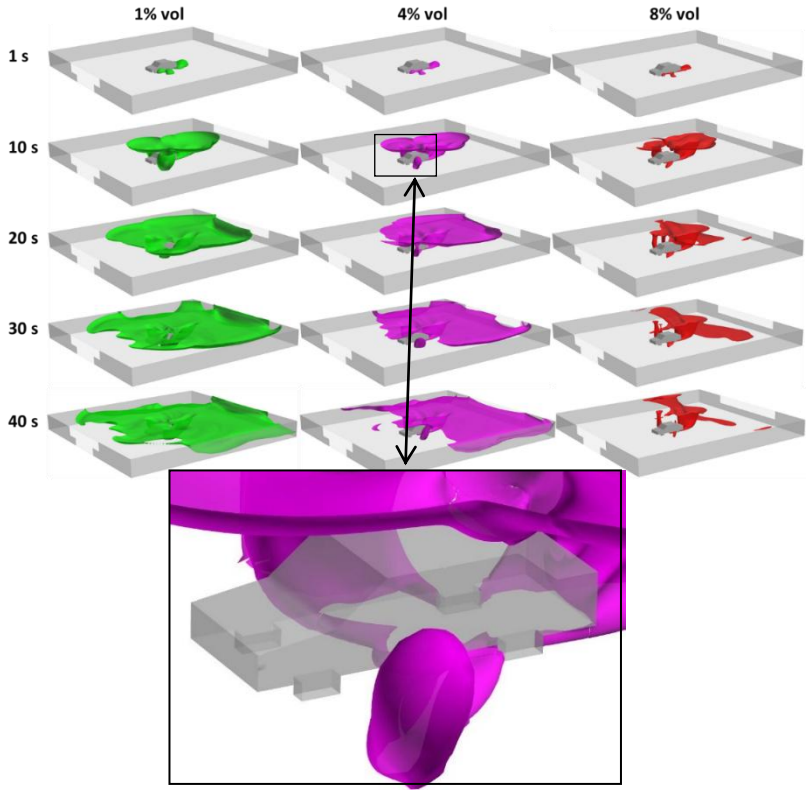

Figure 14. Iso-surface plot of 1%, 4% and 8% vol of hydrogen mole fraction for blowdown from 700 bar through a 2 mm TPRD, 0^o angle downward release.

Figure 15 compares the development of the hydrogen cloud, and spread under the ceiling for downward releases (0^o) through both 2 mm and 0.5 mm TPRD diameters. It can be seen that by decreasing the TPRD diameter from 2 mm to 0.5 mm there will be significant reduction in hydrogen cloud formation around the car and in the carpark with very limited coverage under the ceiling. This is desirable from a safety perspective as it decreases the consequences of ignition and follow-up deflagration. However, tank fire resistance would need to accommodate the longer blowdown period or explosion free in a fire tank should be used. Downward releases through both a 2 mm and 0.5 mm TPRD diameter with angle 0^o led to the formation of flammable hydrogen cloud under the car and and in the vicinity of the doors. Whilst these were of short duration and disperse quickly they present

concerns if ignited. Thus, alternative release angles were considered, as discussed in the next paragraphs.

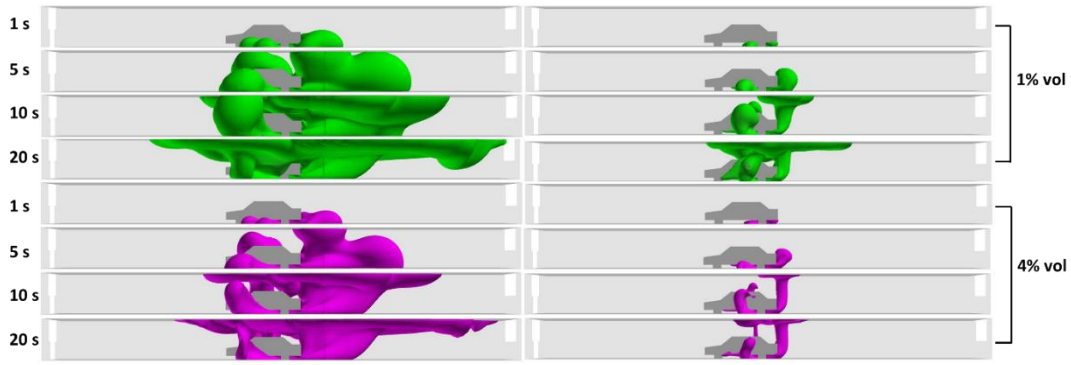

Figure 15. Side view of iso-surface plots for 1% and 4% vol of hydrogen mole fraction for case 4 (2 mm TPRD, left) and case 9 (0.5 mm TPRD, right) with 0^o angle downward release and tank blowdown.

Iso-surfaces of 1%, 4% and 8% for blowdown from 700 bar through a 2 mm TPRD at an angle of 30^o downward (case 5) are shown in Fig. 16. It can be seen how for this angle, hydrogen gas is directed towards the backside of the car. This is a considerable advantage compared with the release at 0^o downward since the driver and passenger escape route are not surrounded by flammable gas. In just 20 s of the release, the back vent of the car park was fully covered with 1% and 4% vol of hydrogen, which does not comply with the ISO/DIS 19880-1 [13], NFPA 2 [14] and IEC (60079-10) [15] standards, which recommend concentrations at the vent areas and escape routes should not exceed 1% vol. This would indicate that based on the current standards a TPRD diameter of 2 mm is unacceptable. Concentrations of 8% vol are only observed at the back of the car attached to the floor. The region at 8% vol reached a maximum in 15 s then decreased. The zoom-set illustrates how the flammable jet was directed away from the car for a downward release angle of 30^o.

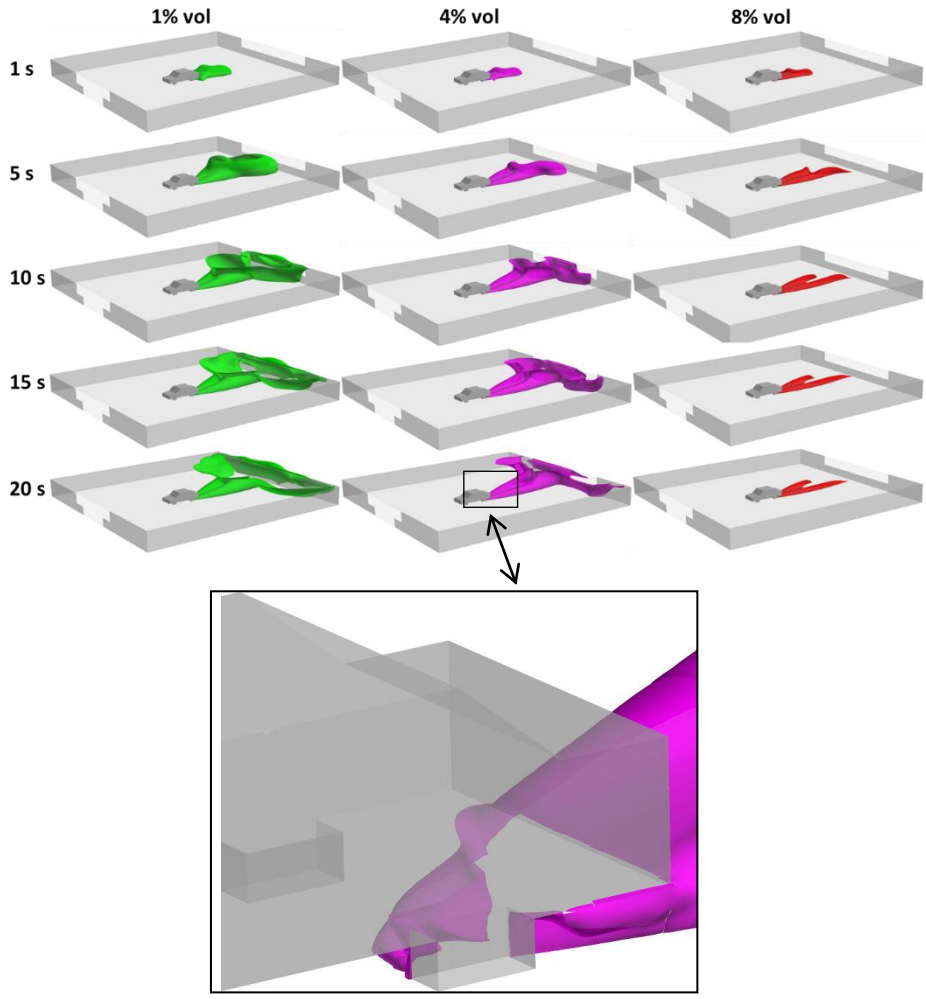

Figure 16. Iso-surface plot of 1%, 4% and 8% vol of hydrogen mole fraction for unignited release of case 5 (2 mm TPRD, 30^{o} angle downward release with tank blowdown).

Figure 17 shows iso-surfaces of 1%, 4% and 8% vol hydrogen, again for a 0^{o} angle downward release but through a 0.5 mm diameter TPRD (case 10). The reduced diameter to 0.5 mm meant the flammable cloud of 4% vol hydrogen reached its maximum coverage area of about 7 m in just 10 s and then decreased to a 6 m tail behind the car. Concentrations of 8% can be observed in the vicinity of the leak with a 1.5 m jet attached to the floor. The cloud envelope of 1% vol was directed to the back vent.

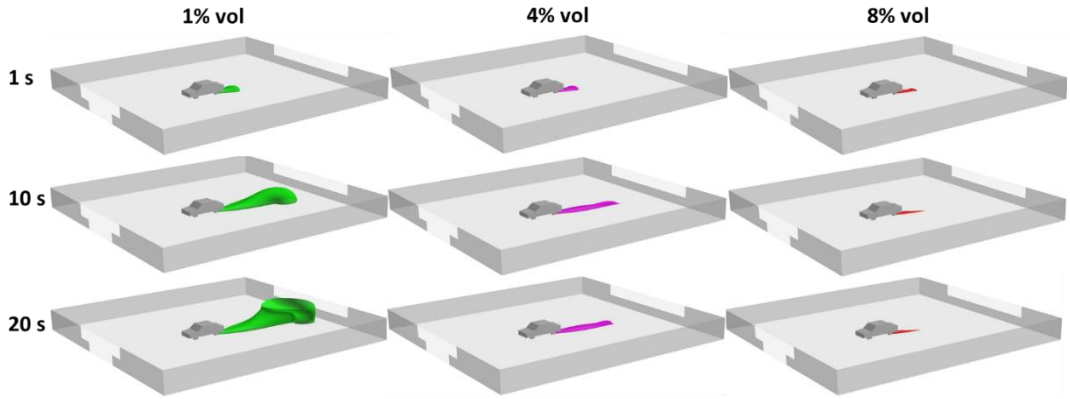

Figure 17. The iso-surface plot of 1%, 4% and 8% vol of hydrogen mole fraction for unignited release of case 10 (0.5 mm TPRD, 30^{o} angle downward release with tank blowdown).

In order to draw a better comparison between the 2 diameters for a 30^{o} angle downward release iso-surface plots are shown in Fig. 18. A significant reduction in the flammable cloud can be noticed when the TPRD diameter is decreased to 0.5 mm.

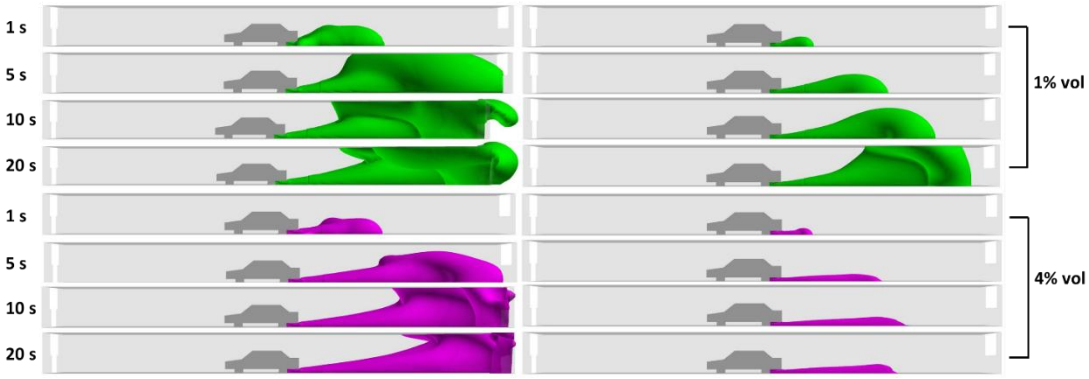

Figure 18. Side view of iso-surface plots for 1% and 4% vol of hydrogen mole fraction for case 5 (2 mm TPRD) (left) and case 10 (0.5 mm TPRD) (right) with 30^{o} angle downward release and tank blowdown.

Finally, a downward angle of 45^{o} was considered. Figures 19 and 20 show the iso-surfaces for 1%, 4% and 8% vol hydrogen for releases though 2 mm and 0.5 mm TPRD respectively. For a TPRD or 2 mm the flammable cloud is tailed back from the car to the back vent opening, and concentrations of 1% vol are observed over the entire back vent.

A longer flow time is shown for the 0.5 mm diameter release to show the effect of tank blowdown on hydrogen cloud formation. Again, the gas clouds are directed backward from the vehicle. A cloud at 1% vol covered the region between the back of the car and the back vent, reaching a maximum volume within 30 s decreasing by 40 s. The results indicate that lower TPRD diameters should be implemented for hydrogen vehicles, if in combination with increased tank fire resistance for safer use in a covered car park with natural ventilation. A side view of iso-surface plots is shown in Fig. 21 to emphasize on

importance of using a smaller TPRD diameter. It can be observed that the 4% vol hydrogen envelope is mainly attached to the floor and directed to the back vent rather than accumulating close to the ceiling. The 1% vol envelope covers the back of the carpark in the 2 mm diameter case.

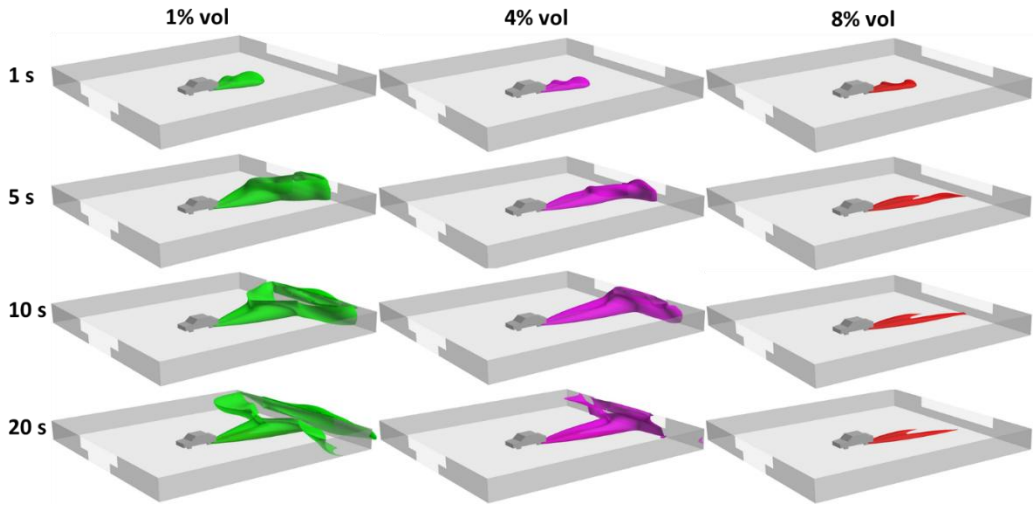

Figure 19. Iso-surface plot of 1%, 4% and 8% vol of hydrogen mole fraction for case 6 (2 mm TPRD, 45^{o} angle downward release with tank blowdown).

.

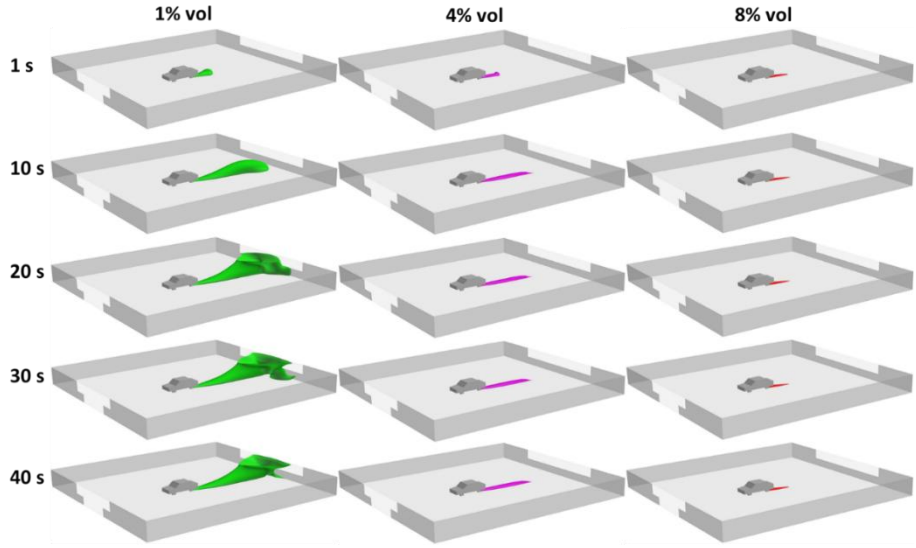

Figure 20 Iso-surface plot of 1%, 4% and 8% vol of hydrogen mole fraction for case 11 (0.5 mm TPRD, 45^{o} angle downward release with tank blowdown).

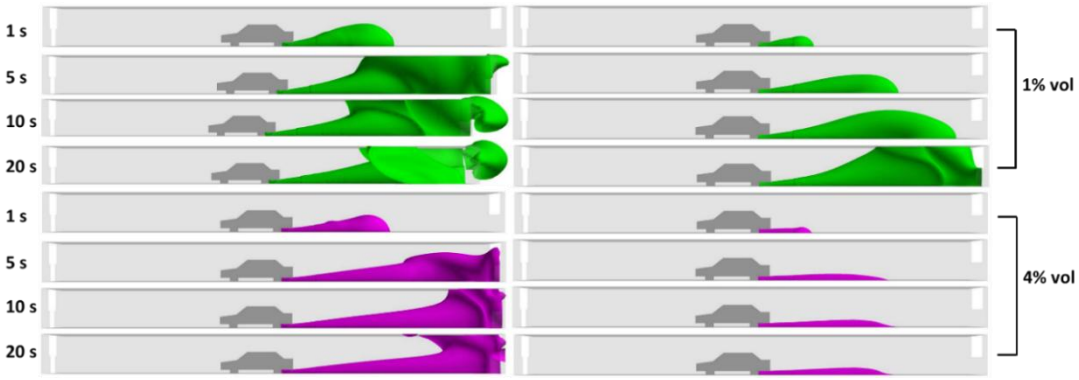

Figure 21. Side view of 1% and 4% vol of hydrogen mole fraction for case 6 (2 mm TPRD) (left) and case 11 (0.5 mm TPRD) (right) with 45^{o} angle downward release and tank blowdown.

Iso-surfaces of 1% and 4% vol hydrogen for the two diameters (0.5 mm and 2 mm) and the three release angles (0^{o}, 30^{o} and 45^{o}) are shown together in Fig. 22 for comparison at a time of 20 s. It is clear how reducing TPRD diameter has a significant effect on flammable cloud formation and dispersion. A straight downward release at 0^{o} results in a flammable cloud around the car, whereas an angle of 30^{o} and 45^{o} pushes the flammable hydrogen gas away from the back of the car enabling a clear escape route (doors) for the vehicle users in the event of ignition.

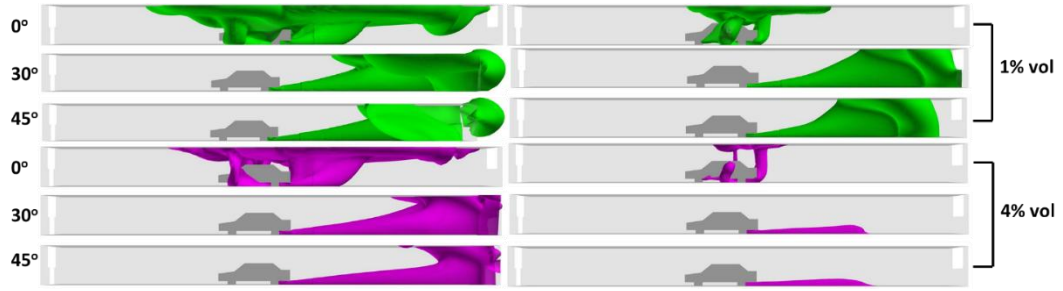

Figure 22 Iso-surface plots of 1% and 4% vol of hydrogen mole fraction for 2 mm TPRD diameter (case 4, 5 and 6) (left) compared to 0.5 mm TPRD diameter (case 9, 10 and 11) (right) for different release direction when flow time is 20 s.

6.0 Conclusions

Unignited hydrogen releases from onboard vehicle storage in a naturally ventilated covered car park has been studied for the first time in this numerical study. Advancing knowledge and understanding in this field is critical to underpin the safe introduction of hydrogen infrastructure, this the study is timely. This novel study presents findings, which are relevant to vehicle manufacturers, standard development organisations (SDOs) and the wider Built Environment. The outcomes indicate that further research of a wider range of scenarios, particularly ignited releases should be undertaken to develop safety guidance for both hydrogen fuel cell vehicles and the associated infrastructure.

The originality of the study has meant that there is an absence of existing experimental data. Thus the numerical model was firstly validated against experimental data of KIT (Germany) on helium impinging jet, and a good numerical and experimental agreement was achieved within an acceptable engineering error. Simulations were carried out for a carpark with dimensions LxWxH=30x28.6x2.6 m, incorporating two vents which provided an opening equivalent in area to 5% of the floor area across two opposing walls in accordance with British Standard BS 7346-7:2013. Eleven release cases from 700 bar storage were considered; four upward releases from a pipe 0.5 m above the floor (no car presence), and an upward and six downward releases where the car geometry was included. The similarity law for unignited jets was used as an additional validation step for upward releases to approximate hydrogen percentages expected in the vicinity of the ceiling. A validated blowdown model, developed at Ulster University, was applied for all scenarios.

As expected, a constant mass flow rate release resulted in a larger flammable cloud within the car park compared to a blowdown release through the same TPRD diameter, demonstrating the importance of including when predicting behaviour in real scenarios. It was demonstrated how a 0.5 mm diameter TPRD resulted in a considerably smaller flammable cloud than that produced by either a 2 mm or 3.34 mm diameter TPRD. Concerns have been previously highlighted for the use of "typical" TPRD diameters in enclosures with relation to the pressure peaking phenomena [10]. This work indicates that safety concerns also exist for "typical" diameters in enclosure scenarios where the ventilation is sufficient to ensure that pressure peaking is not of concern. It has been demonstrated how the diameter should be reduced as much as is reasonably practicable.

In order to investigate a real case scenario, a car body geometry was modelled, and downward and upward releases from 700 bar storage through a 0.5 mm TPRD were compared. The downward release resulted in a larger flammable envelope in the vicinity of the car, particularly surrounding the doors and rear. However, the average hydrogen concentration within the flammable cloud was lower compared with the upward release. In contrast, an upward release led to a greater flammable envelope beneath the ceiling, but not surrounding the car. Both downward and upward releases from 700 bar through a 0.5 mm TPRD in a covered car park can be considered as a safer choice, when coupled with appropriate tank design, producing a limited flammable cloud which disperses quickly. However, the work does indicate that if larger diameter TPRDs are to be used, then safety considerations for an unignited release in a covered car park should be further investigated and addressed. Three (0^o, 30^o and 45^o) different downward release angles were compared to understand the effects of hydrogen release orientation. The straight downward release (zero angle) produced a flammable hydrogen cloud around the car, albeit briefly but this may present challenges for first responders to access the vehicle occupants if it is ignited. Downward releases at angles of 30^o and 45^o toward the back of the car pushed the flammable gas away from the car surroundings, making it safer for users to escape. These factors must be considered in the design of TPRDs for onboard storage in hydrogen vehicles.

7.0 References

[1] W.G. Houf, G.H. Evans, I.W. Ekoto, E.G. Merilo, M.A. Groethe, Hydrogen fuel-cell forklift vehicle releases in enclosed spaces, Int. J. Hydrogen Energy (2013). doi:10.1016/j.ijhydene.2012.05.115.

[2] A.G. Venetsanos, E. Papanikolaou, M. Delichatsios, J. Garcia, O.R. Hansen, M. Heitsch, A. Huser, W. Jahn, T. Jordan, J.M. Lacome, H.S. Ledin, D. Makarov, P. Middha, E. Studer, A. V. Tchouvelev, A. Teodorczyk, F. Verbecke, M.M. Van der Voort, An inter-comparison exercise on the capabilities of CFD models to predict the short and long term distribution and mixing of hydrogen in a garage, Int. J. Hydrogen Energy. (2009). doi:10.1016/j.ijhydene.2009.01.055.

[3] E.A. Papanikolaou, A.G. Venetsanos, M. Heitsch, D. Baraldi, A. Huser, J. Pujol, J. Garcia, N. Markatos, HySafe SBEP-V20: Numerical studies of release experiments inside a naturally ventilated residential garage, Int. J. Hydrogen Energy. (2010). doi:10.1016/j.ijhydene.2010.02.020.

[4] G. Bernard-Michel, B. Cariteau, J. Ni, S. Jallais, E. Vyazmina, D. Melideo, CFD Benchmark Based Exp. Helium Dispers. a 1 M3 Enclos. e Intercomparisons Plume, In: Proceedings of ICHS 2013, Brussels, Belgium, 2013: p. paper ID No. 145.

[5] V. Molkov, V. Shentsov, Numerical and physical requirements to simulation of gas release and dispersion in an enclosure with one vent, Int. J. Hydrogen Energy. (2014). doi:10.1016/j.ijhydene.2014.06.154.

[6] B. Cariteau, I. Tkatschenko, Experimental study of the effects of vent geometry on the dispersion of a buoyant gas in a small enclosure, Int. J. Hydrogen Energy. (2013). doi:10.1016/j.ijhydene.2013.03.100.

[7] V. Molkov, Hydrogen non-reacting and reacting jets in stagnant air: overview and state of the art, Proceedings of the 10th International Conference on Fluid Control, Measurement, and Visualization (FLUCOM2009), 17-21 August 2009. Moscow, Russia.

[8] V. Molkov, Fundamentals of Hydrogen Safety Engineering I, www.bookboon. com, 2012.

[9] Z.Y. Li, D. Makarov, J. Keenan, V. Molkov, CFD study of the unignited and ignited hydrogen releases from TPRD under a fuel cell car, Proceedings of ICHS 2015, Paper No.322.

[10] S. Brennan, H. G. Hussein, D. Makarov, V. Shentsov, V. Molkov, Pressure effects of an ignited release from onboard storage in a garage with a single vent, Int. J. Hydrogen Energy. (2018). https://doi.org/10.1016/j.ijhydene.2018.07.130.

[11] S. Brennan, V. Molkov, Safety assessment of unignited hydrogen discharge from onboard storage in garages with low levels of natural ventilation, Int. J. Hydrogen Energy. (2013). doi:10.1016/j.ijhydene.2012.08.036.

[12] D. Makarov, V. Shentsov, M. Kuznetsov, V. Molkov, Pressure peaking phenomenon: model validation against unignited release and jet fire experiments, Int. J. Hydrog. Energy. (2018) Volume 43, Issue 19, 10 May 2018, Pages 9454-9469

[13] S. Brennan, D. Makarov, V. Molkov, Dynamics of Flammable Hydrogen-Air Mixture Formation in an Enclosure with a Single Vent, Sixth Int. Semin. Fire Explos. Hazards. (2011) 978–981. doi:10.3850/978-981-08-7724-8.

[14] International Electrotechnical commission IEC 60079-10-1, Explosive atmospheres - Part 10-1: Classification of areas - Explosive gas atmospheres, 2015.

[15] National fire protection association NFPA 2, Hydrogen technologies code, 2011.

[16] The International organization for standardization ISO/DIS 19880-1, Gaseous hydrogen – fuelling stations, Part 1: General requirements, 2018.

[17] W.K. Chow, On safety systems for underground car parks, Tunn. Undergr. Sp. Technol. (1998). doi:10.1016/S0886-7798(98)00060-1.

[18] M.G.M. van der Heijden, M.G.L.C. Loomans, A.D. Lemaire, J.L.M. Hensen, Fire safety assessment of semi-open car parks based on validated CFD simulations, Build. Simul. (2013). doi:10.1007/s12273-013-0118-7.

[19] X.G. Zhang, Y.C. Guo, C.K. Chan, W.Y. Lin, Numerical simulations on fire spread and smoke movement in an underground car park, Build. Environ. (2007). doi:10.1016/j.buildenv.2006.11.002.

[20] L. Joyeux, D., Kruppa, J., Cajot, L.G., Schleich, J.B., Van de Leur, P. and Twilt, Demonstration of real fire tests in car parks and high buildings., 2002.

[21] British Standard institution BS 7346-7:2013, Components for smoke and heat control systems – Part 7: Code of practice on functional recommendations and calculation methods for smoke and heat control systems for covered car parks, 2013.

[22] Nederlands Normalisatie-Instituut NEN 2443. parkeren en stallen van personenauto's op terreinen en garages, ICS 91.040.99, 2000.

[23] V. Molkov, D. Makarov, M. Bragin, Physics and modelling of underexpanded jets and hydrogen dispersion in atmosphere, in: 2009.

[24] ANSYS Fluent R16.2 User Guide, (2016).

[25] H. G. Hussein, S. Brennan, D. Makarov, V. Shentsov, V. Molkov, Numerical validation of pressure peaking from an ignited hydrogen release in a laboratory-scale enclosure and application to a garage, Int. J. Hydrogen Energy. (2018).

[26] T.-H. Shih, W.W. Liou, A. Shabbir, Z. Yang, J. Zhu, A new k-ϵ eddy viscosity model for high Reynolds number turbulent flows, Computers Fluids. 24 (1995) 227–238. doi:10.1016/0045-7930(94)00032-T.

[27] S.B. POPE, An explanation of the turbulent round-jet/plane-jet anomaly, AIAA J. (1978). doi:10.2514/3.7521.

[28] D.M.C. Cirrone, D. Makarov, V. Molkov, Simulation of thermal hazards from hydrogen under-expanded jet fire. Int. J. Hydrogen Energy. (2018).

[29] P.T. Roberts, L.C. Shirvill, T.A. Roberts, C.J. Butler, M. Royle, Dispersion of hydrogen from high-pressure sources, in: Inst. Chem. Eng. Symp. Ser., 2006: p. 410.

[30] D. Baraldi, D. Melideo, A. Kotchourko, K. Ren, J. Yanez, O. Jedicke, S.G. Giannissi, I.C. Tolias, A.G. Venetsanos, J. Keenan, D. Makarov, V. Molkov, S. Slater, F. Verbecke, A. Duclos, The CFD Model Evaluation Protocol, 2016.

[31] M. Dadashzadeh, D. Makarov, V Molkov, Non-adiabatic blowdown model: a complementary tool for the safety design of tank-TPRD system, In: Proceedings of ICHS 2017, Hamburg, Germany, 2017.

[32] S. Brennan, V. Molkov, Pressure peaking phenomenon for indoor hydrogen releases, International Journal of Hydrogen Energy. 43, 39, p. 18530-18541 12 p.

[33] J. Wen, Experimental validation of volumetric source model in CFD applications for high-pressure hydrogen jet impingement (Project 2081), project report presentation, 2015.

[34] Hao, D., Wang, X., Zhang, Y. et al. Experimental Study on Hydrogen Leakage and Emission of Fuel Cell Vehicles in Confined Spaces. Automot. Innov. (2020). https://doi.org/10.1007/s42154-020-00096-z